Computer Simulation of Proton Transfers of Small Acids in Water

S. R. Billeter and W. F. van Gunsteren*

Physical Chemistry, ETH Zentrum, CH-8092 Zürich, Switzerland

Received: November 18, 1999; In Final Form: January 18, 2000

The potential experienced by an excess proton from the acetate ion solvated in water has been investigated, and a parameter set is presented which is suitable for molecular dynamics (MD) or mixed MD/quantum dynamics (QD) simulations and compatible with the GROMOS96 force field. A general procedure for deriving parameters for the proton potential is presented. The simulations started from five random configurations, energy minimized and equilibrated in both the deprotonated and the protonated state. In the case of weak acids such as the considered molecules, the proton transfer rate of both deprotonation and protonation of the solvated acid has been found to be considerably lower than the corresponding proton transfer rates between neighboring water molecules. The reaction free energy profile of a proton transfer reaction has been determined using umbrella sampling and thermodynamic integration. The results encourage the application of the mixed MD/QD simulation scheme to simulations of proton transfers from and to large biomolecules in water.

I. Introduction

All living cellulae have to regulate their p*H* within some tenths, and the structure of biomolecules often depends strongly on the p*H* of their environment. However, in molecular dynamics (MD) simulations of biomolecules the state of protonation of the protonizable sites is generally chosen fixed according to a particular p*H* value and the effects of the changing local environment on the protonation of a particular site are neglected. Moreover, most simulations of biologically relevant systems are carried out without any possibility of proton transfer at all. There are two reasons for that: (1) no general empirical force fields for transferable protons are available and the specific models that have been proposed are computationally expensive due to the impossibility of expressing the potential in terms of additive pair potentials; (2) the inclusion of electronic degrees of freedom in a simulation to find the forces acting on the protons has only very recently become possible.[1−3]

While ab initio MD methods such as Car−Parrinello are able to model proton transfer reactions very accurately,[3,4] empirical potential energy surfaces (PES) are computationally much cheaper and therefore make it possible to sample a larger part of the configurational space at the expense of a somewhat reduced accuracy. Among the empirical PES for proton transfers, the dissociable water models, where the protons are not explicitly bound to individual molecules (see, e.g., refs 5, 6), are difficult to combine with existing force fields for biomolecular systems. Empirical valence bond (EVB) methods[7] have been applied very sucessfully to simulate proton transfers in water.[8−10] Following the philosophy of the GROMOS96[11,12] force field, we use the parameters for the protonated and the deprotonated state of a given molecule or residue applying the GROMOS96 machinery for the perturbation of a Hamiltonian. The forces for binding a proton to its acceptors are described using pair and triple terms.[13] As pointed out in refs 13 and 14, it is problematic to use high quality ab initio calculations to derive the parameters for these terms, and thus empirical values are used. There are close relationships between the EVB and the force field approaches: The role of the off-diagonal elements of the EVB Hamiltonian to be diagonalized is taken over by the proton−acceptor−acceptor triple terms, and for each reference structure forming the EVB basis, an "acidic" transferable proton is chosen in the force field approach.

The program package QDGROMOS is an extension of the biomolecular simulation package GROMOS96[11,12] for non-adiabatic mixed MD/QD simulations of proton transfers. The aim of the programs of QDGROMOS,[15] the protonizable extended simple point charge (SPC/E) model for liquid water[13] and the proton transfer simulations of small acids in water described in the current article is to explore and establish procedures of setting up mixed quantum dynamics (QD)/molecular dynamics (MD) simulations of biomolecules such as proteins or nucleic acids with protonizable sites in aqueous solution.

Related methods for studying the quantum dynamics of proton transfers in a classically treated environment are among others "quantum-classical molecular dynamics",[16] "density matrix evolution",[17] "surface hopping" techniques,[18,19] and semiclassical quantum dynamics.[20] The surface hopping and semiclassical techniques work around problems occurring with mixed states in the regime of weakly coupled adiabatic energy surfaces, and it is planned to apply surface hopping in this regime as suggested by ref 21 using the readily available adiabatic basis for the proton(s) in QDGROMOS.

II. Interaction Models

All MD simulations have been carried out using QDGROMOS, a program for non-adiabatic mixed QD/MD proton transfer simulations. It is based on GROMOS96[11,12] and has been described in a preceding article.[15] Figure 1 shows the geometric elements of the proton-bound acetic acid−water dimer except for the proton−oxygen−carbon−oxygen dihedral angle. The functional form of the proton potential in liquid SPC/E

* Corresponding author.

10.1021/jp994127q CCC: $19.00
Published on Web 04/13/2000

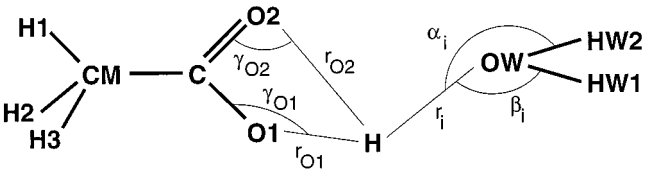

Figure 1. The geometric elements of a proton-bound acetic acid−water pair. The atoms can be classified into four groups: the proton (H), the protonizable water molecule (OW, HW1, HW2), the atoms of protonizable groups of the acid (O1, C, O2), and the non-protonizable atoms of the acid (CM, H1, H2, H3).

water has been described in refs 13 and 15. It can be summarized as follows. The pair interaction V_p is

$$V_p = \sum_i [V_{rad}(r_i) + V_{ang}(r_i,\alpha_i,\beta_i)] \quad (1)$$

the terms representing the interaction between the proton and the water molecule *i*. They consist of a monopole−dipole term V_{rad},

$$V_{rad}(r) = \frac{1}{4\pi\epsilon}\frac{qm}{(r + r_{off})^2} \quad (2)$$

and an angular term V_{ang}:

$$V_{ang}(r,\alpha,\beta) = \exp\left(-\frac{r}{\rho_{ang}}\right) \times b_2[(\cos(\alpha) - \cos(tet.))^2 + (\cos(\beta) - \cos(tet.))^2] \quad (3)$$

defined in terms of the geometric elements shown in Figure 1, and cos(*tet.*) denotes the cosine of a tetrahedral angle. The water−proton−water triple interaction V_t is

$$V_t = \sum_i V_{lj}(r_i,s\lambda_i) + \sum_{i,k_i}\sum_{j,l_j} V_{pol}(r_{k_i l_j},r_i,r_j) \quad (4)$$

The first term involving the distance r_i between the proton and the oxygen of water molecule *i*, and the distance r_j between the proton and the oxygen of water molecule *j* consists of a Lennard−Jones term V_{l_j} for the distance r_i:

$$V_{lj}(r_i,s\lambda_i) = 4\epsilon(s\lambda_i) \times [(\sigma(s\lambda_i)/r_i)^{12} - (\sigma(s\lambda_i)/r_i)^6] \quad (5)$$

whose parameters ϵ and σ depend on the distances r_j,

$$\epsilon(\lambda) = (1 - \lambda)\epsilon_0 + \lambda\epsilon_1 \quad (6)$$

$$\sigma(\lambda) = (1 - \lambda)\sigma_0 + \lambda\sigma_1 \quad (7)$$

$$s\lambda_i = \sum_{j\neq i}\lambda_j \quad (8)$$

$$\lambda_j = \begin{cases} 1 \text{ if } r_j < r_0 \\ 0 \text{ if } r_j > r_1 \\ \frac{1}{4}(1 + \cos[\pi * (r_j - r_0)/(r_1 - r_0)])^2 \text{ otherwise} \end{cases} \quad (9)$$

with ϵ_0, ϵ_1, σ_0, σ_1, r_0, and r_1 as fixed parameters. The second term consists of a polarization potential V_{pol}:

$$V_{pol}(r_{k_i l_j},r_i,r_j) = \frac{1}{4\pi\epsilon}\frac{q_{k_i}(r_i)q_{l_j}(r_j) - q^\infty_{k_i}q^\infty_{l_j}}{r_{k_i l_j}} \quad (10)$$

using variable charges q_{k_i}, q_{l_j} on the atoms k_i and l_j of the molecules *i* and *j*, adiabatically depending on the distances r_i and r_j between the proton and the oxygen atoms of molecules *i* and *j*. $r_{k_i l_j}$ denotes the distance between atoms k_i and l_j. The functional form of the charges is

$$q_{OW}(r) = q^\infty_{OW} + \Delta q_{ovl}(r) - 2\Delta q_{pol}(r) \quad (11)$$

$$q_{HW}(r) = q^\infty_{HW} + \Delta q_{pol}(r) \quad (12)$$

$$q_{H^+}(\{r_i\}) = q^\infty_{H^+} - \sum_i \Delta q_{ovl}(r_i) \quad (13)$$

$$\Delta q_{ovl}(r) = \Delta q_{ovl} \times \exp\left(-\frac{r}{\rho_{ovl}}\right) \quad (14)$$

$$\Delta q_{ovl}(r) = \Delta q'_{pol} \times \frac{\rho^2_{pol}}{r^2} = \Delta q_{pol} \times \frac{1}{r^2} \quad (15)$$

The potential function for the protonizable atom groups of other molecules than water (e.g., an acid) consists of four parts. The first part is the equivalent of the terms of eqs 4−10, but with the protonizable group *i* playing the role of water molecule *i*. So, the angle γ_i plays the role of angle α_i, and β_i has no equivalent (Figure 1). The second part concerns the proton−protonizable group pair potential energy V_p. Since often the deprotonated form of an acid is charged, monopole−monopole interactions are required,

$$V_{rad}(r) = \frac{1}{4\pi\epsilon}\left[\frac{qm}{(r + r_{off})^2} + \frac{qq}{r + r_{off}}\right] \quad (16)$$

Both parameters *qm* and *qq* do not depend on the reaction coordinates: they are responsible for the long-range region of the proton−protolyte interactions. Out-of-plane dihedral interactions as described in ref 11, eq 2.5.4.1, multiplied by the same exponential prefactor as used in eq 3, are added to the angular term V_{ang}. The third part consists of standard bonded and non-bonded interaction terms as used in the empirical GROMOS96[11] force field. The atomic charges, ideal bond lengths, bond angles, and dihedral angles as well as their force constants are given by the GROMOS96 force field, both for protonated and deprotonated states. The actual value of these force field parameters depends on the distance between the protonizable sites of the acid (the protonizable atom group) and the proton, linearly interpolated using the reaction coordinates λ_i introduced in eq 9. The ideal bond length b_{CO1} between oxygen O1 and carbon C (see Figure 1) depends, e.g., on the distance between the proton and the oxygen atom O1,

$$b_{CO1} = (1 - \lambda_{O1})b^{\text{depr}}_{CO1} + \lambda_{O1}b^{\text{prot}}_{CO1} \quad (17)$$

and the bond-stretching energy between atom O1 and C has non-zero gradient components to the atoms H, O1, and C. The charge q_C on the carbon atom C depends on the distances between the proton and the oxygen atoms O1 and O2,

$$q_C = (1 - \lambda_{O1} - \lambda_{O2})q^{\text{depr}}_C + (\lambda_{O1} + \lambda_{O2})q^{\text{prot}}_C \quad (18)$$

and the electrostatic energy between atom C and another, non-polarizable atom X has non-zero gradient components to the atoms H, O1, O2, C, and X. The functional form of the potential energy terms involving the proton and the atoms of a protonizable atom group (e.g., an acid) arising from variable charges,

TABLE 1: Binding Energies in Hartree of Some Clusters Containing Protolytes in Vacuo at MP2/6-31G Level[a]**

	acid monomer	acid−water dimer	
acid	base + proton	base + proton + water	acid + water
hydroxide ion	−0.69372	−0.70495	−0.01123
water	−0.28633	−0.34901	−0.06268
formate	−0.58436	−0.60650	−0.02215
acetate	−0.58987	−0.61199	−0.02212

[a] The basis set superposition error has not been corrected. The energy of the cluster in the upper line of the heading has been compared to the sum of the energies of the fragments listed in the lower line of the heading.

bonds, bond angles, dihedrals, and out-of-plane dihedrals is the same as for the GROMOS96 perturbation.[11] Note that the electrostatic potential energy between an atom with a charge depending on the distance to a proton and any other atom has gradient components with respect to the proton coordinates as well.[13] Lennard−Jones parameters of the GROMOS96 non-bonded interaction terms, influencing only the immediate neighborhood of an atom, are kept constant at the values of the deprotonated state. To satisfy charge conservation, the charge of the proton q_p is

$$q_p = q_p^{\mathrm{depr}} - \sum_{i,k_i} \lambda_i (q_{k_i}^{\mathrm{prot}} - q_{k_i}^{\mathrm{depr}}) \qquad (19)$$

where $q_p^{\mathrm{depr}} = q_p^{\infty}$ is by definition equal to 1*e*. The adiabatic polarization and charge overlap terms of the protonizable SPC/E water model[13] are given by eqs 11−15. They have not been adapted to conform to equations 18 and 19, but their computation is compatible. The generalization to more than one proton is straightforward except for the dependence of the charges on the states of the protons in case of a product state representation of the quantum dynamical protons. This has been discussed in detail in section 2.7.3 of ref 15. The fourth part has already been mentioned in ref 13: the electrostatic interactions between the proton(s) and all atoms which do not belong to a protonizable group (Figure 1) have spatial derivatives with respect to the positions of atoms belonging to a protonizable group due to eq 19.

Since the binding energies involved with proton transfers (e.g., $\epsilon_0 = 1149.97$ kJ/mol for acetic acid, parameter set a8) exceed the intermolecular binding energies (e.g., $\epsilon_{\mathrm{OW-OW}} = 0.6502$ kJ/mol for water oxygen−water oxygen, GROMOS96) by orders of magnitude, and the length scales are much smaller, ($\sigma_0 = 0.09$ nm, $\sigma_{\mathrm{OW-OW}} = 0.3166$ nm), the forces can be expected to be much larger, and much smaller time steps are required. A variable time step algorithm aimed at decreasing the sometimes huge pulses arising from the repulsive part of the Lennard−Jones potential has been described in section II.D of ref 13. Another possibility to alleviate the necessity to use small time steps is to change the shape of the Lennard−Jones function itself: one could think of using smaller negative exponents over the entire range of distances or in the repulsive region only ($r < r_b = \sigma \times 2^{1/6}$), or of using other soft-core potentials, e.g., eq 2.5.6.9.1 of ref 11.

The molecular orbital calculations for Table 1 have been carried out at MP2/6-31G** level using the Gaussian94 package.[22] The basis set superposition error was not corrected. All MD and QD/MD simulations have been carried out at 300 K. A Berendsen thermostat[23] with a coupling time of 0.4 ps has been used to keep the temperature constant in the simulations of the solution, and periodic boundary conditions of a truncated octahedron with a box length of 2.36556 nm have been applied. The one-dimensional representation of the proton used 64 basis points, spanned between the oxygen atom O1 of the acetic acid molecule and the oxygen atom OW of a water molecule. The proton potential of the acid−water dimer including GROMOS96 interactions has been calculated and plotted using the program Maple V, version 3.[24]

III. The Shape of the Hydrogen Bond Potential

For acetic acid, the parameter set "ac4", adjusted to approximately match the values in Table 1, is taken as a starting point. Its values are listed in Table 2, and Figure 2 shows the shape of the resulting proton potential as a function of different distances and angles. The force constants for angular and tetrahedral interactions come from the standard GROMOS96 force field parameter set and should not be changed. Since the monopole−dipole and the monopole−monopole interaction terms (eq 16) have the most global effect, their parameters *qm* and *qq* need to be chosen first. The monopole−monopole interactions have been switched off in parameter set "ac4". The use of the reaction coordinate λ from eq 9 as one coordinate for all interaction terms involving triples of a proton and two

TABLE 2: Parameters for the Protonizable SPC/E Water[13] and the Acetic Acid Models "ac4", "a8", and "a9" Which Complement the SPC/E Water Model Parameters (which are part of the GROMOS96 force field[11]) and the Parameters for Acetic Acid and the Acetate Ion of the GROMOS96 Force Field[a]

			acetic acid			
parameter	meaning	pSPC/E	ac4	a8	a9	unit
qq	proton charge times residue charge		0.0	0.4	0.4	e^2
qm	proton charge times dipole moment	0.3	0.2	0.2	0.2	e^2 Å
r_{off}	offset distance for monopole-dipole interactions	0.4	0.4	0.4	0.4	Å
ρ_{ang}	angular interaction decay length	1.0	1.0	1.0	1.0	Å
b_2	angular force constant(s)	0.280	0.17140*	0.17140*	0.17140*	Hartree
r_0	proton−acceptor distance, protonated state	1.0	1.0	1.0	1.0	Å
r_1	proton−acceptor distance, deprotonated state	1.8	2.4	1.8	1.8	Å
σ_0	Lennard−Jones distance, proton free	0.9	0.9	0.9	0.9	Å
σ_1	Lennard−Jones distance, proton bound	1.1	1.20	1.05	1.05	Å
ϵ_0	Lennard−Jones energy, proton free	0.180	0.542	0.438	0.219	Hartree
ϵ_1	Lennard−Jones energy, proton bound	0.108	0.100	0.050	0.050	Hartree
Δq_{ovl}	overlap charge	18.3923				e
Δq_{pol}	polarization charge	0.1562				e Å^2
ρ_{ovl}	polarization decay distance	0.2646				Å

[a] "Proton bound" means that another proton acceptor than the oxygen atom under consideration is closer to the proton than the distance r_0 ($s\lambda$=1), see eqs 8 and 9. The asterisk indicates that the angular force constant is equal to the GROMOS96 parameter for the protonated molecule.

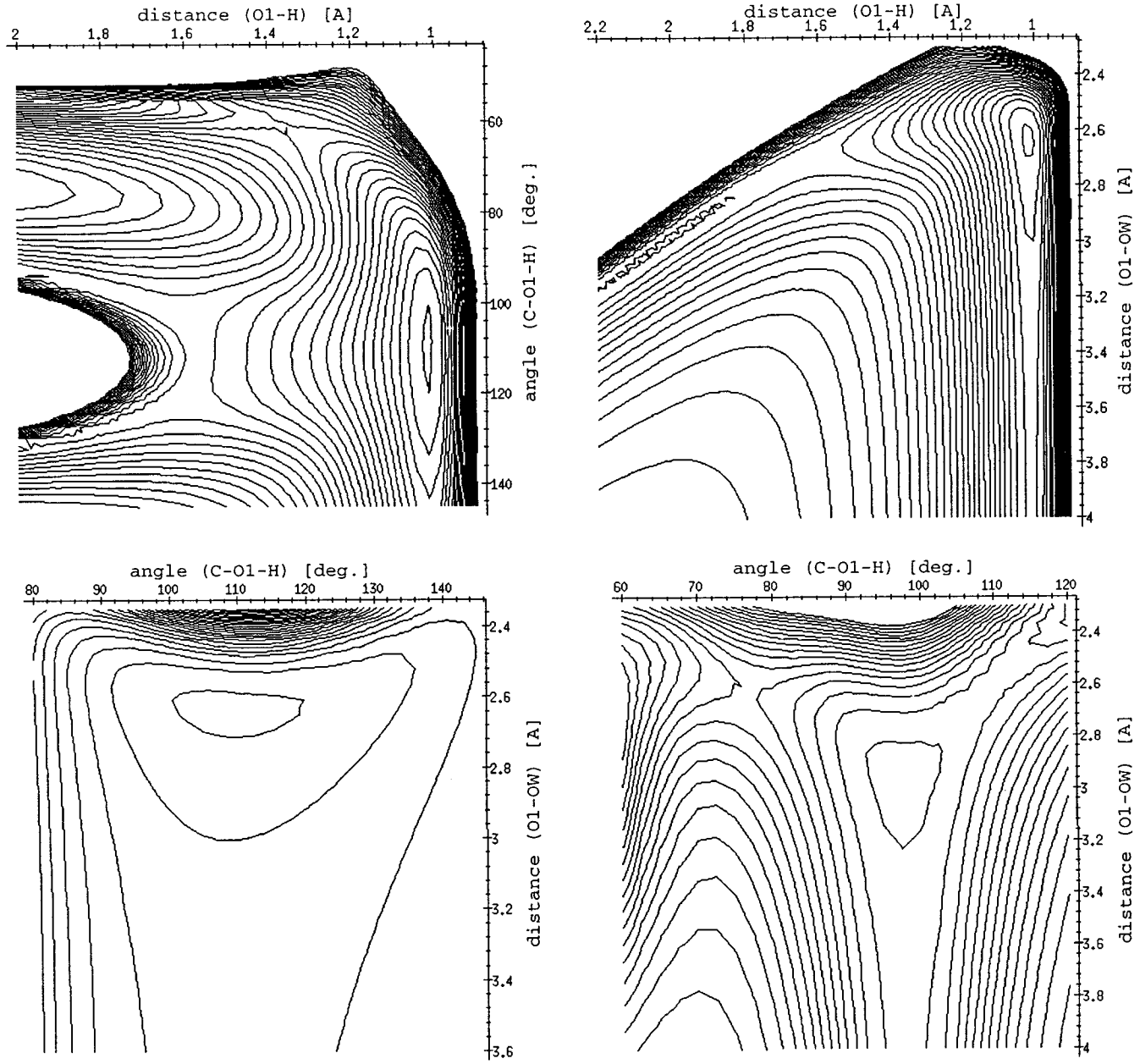

Figure 2. Potential energy contours in Hartree for the proton in the acetic acid−water dimer shown in Figure 1 including the GROMOS96 interaction using the parameter set "ac4" (see Table 2) as a function of the distances *r* between the oxygen atom O1 and the proton H and between the oxygen atom O1 and the water oxygen atom OW, and of the angles *a* between carbon C, oxygen O1, and the proton H and between carbon C, oxygen O1, and oxygen OW. Left side, top: r(O1−OW) = 2.64 Å, a(C−O1−OW) = 112.0°; left side, bottom: r(O1−H) = 1.02 Å, a(C−O1−OW) = 112.0°; right side, top: a(C−O1−H) = 108.0°, a(C−O1−OW) = 112.0°; right side, bottom: r(O1−H) = r(O1−OW) − 1.01 Å, a(C−O1−OW) = 98.0°. The equidistance between the contours is 0.033 Hartree.

other atoms instead of using the distance from the proton to both interacting partners reduces the interdependence of the parameters considerably, and the dependence of the shape of the proton potential on each parameter can be described roughly as in the column "meaning" of Table 2. Details about the equilibrium geometries and energies in vacuo resulting from the different parameter sets are given in ref 14.

As a result of the current and the next sections, the following procedure for finding proton potential parameters and setting up a proton transfer simulation is proposed (see also Figure 3; the meaning of the symbols is described in Section II and Table 2):

1. Prepare a molecular topology of the protonated and the deprotonated form of the acid including the proton in both cases.

2. Find at least five random configurations of the solvated acid and carry out classical energy minimizations using the two molecular topologies and distance restraints for the deprotonated state to "attach" the proton to a solvent molecule. The terms are switched on in the following order: 1. bonded, 2. Lennard−Jones, 3. electrostatics, 4. periodic boundary conditions without electrostatics, 5. periodic boundary conditions including electrostatics. The obtained configurations are then equilibrated by MD simulation for at least 40 ps using 0.1 ps as relaxation time for the Berendsen thermostat.[23]

3. Do ab initio calculations for the acid−water dimer in the protonated and in the deprotonated form. Use as few constraints as possible.

4. Start from an existing parameter set, e.g., acetic acid, "a8".

5. Adjust the parameters *qm* and *qq* which govern the monopole−dipole and the monopole−monopole interaction

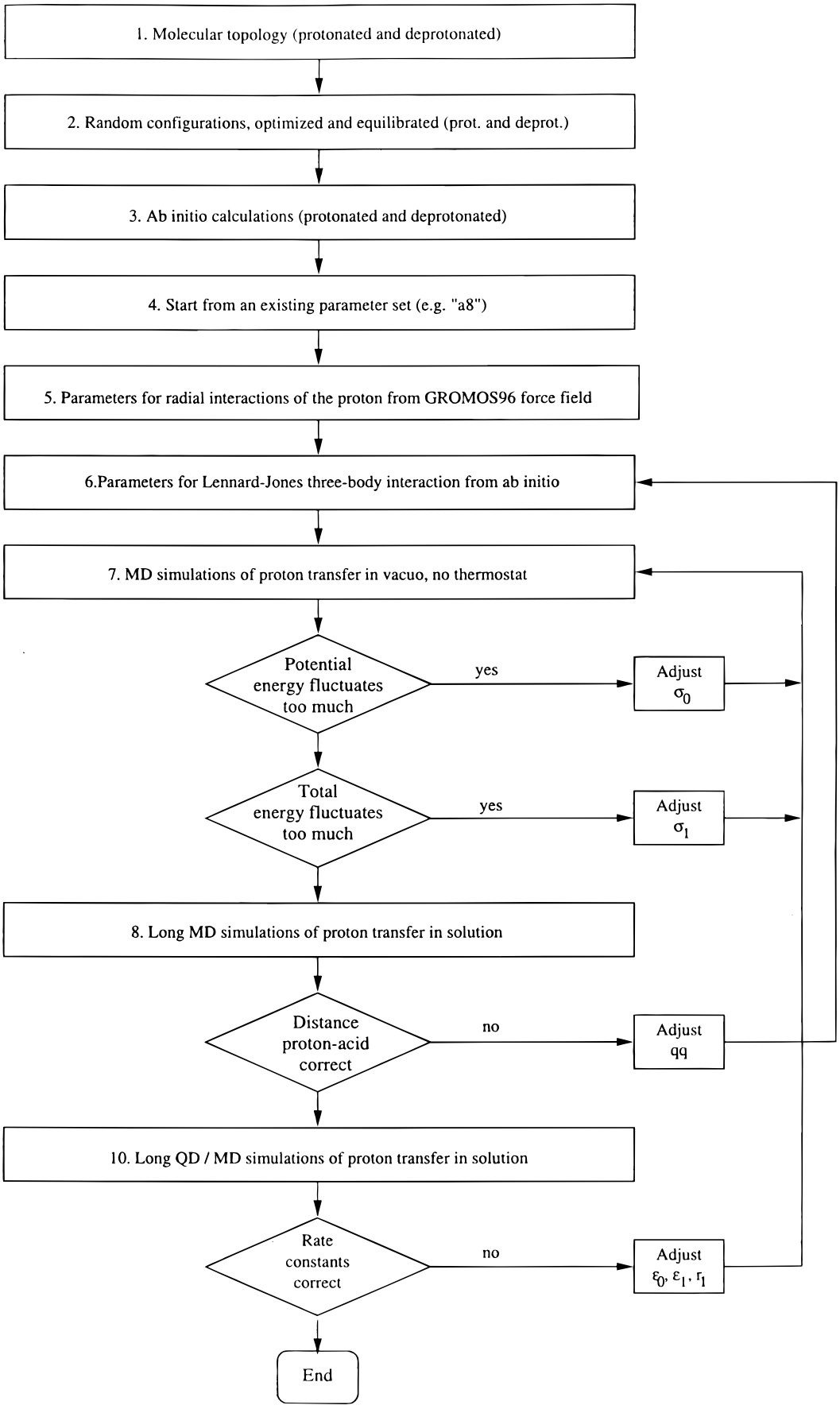

Figure 3. Flow chart of the procedure for finding proton potential parameters described in Section III.

(eq 16), starting from values taken from the GROMOS96 force field.

6. Adjust the parameters σ_0 and ϵ_0 (eqs 6 and 7) to reproduce the position and the depth of the potential well near the proton

TABLE 3: MD Simulations of Acetic Acid in 216 Water Molecules over 1 ps Using the Proton Potential Parameter Sets "a8" and "a9" (see Table 2) and Different Initial Configurations at 300 K[a]

set	configuration	total energy kJ mol^{-1}	reaction rate ps^{-1}	fraction of time	proton−oxygen dist. nm/1
a8	opt.	−11129/25	0.0	1.000	
a8	prot.	−11167/33	0.0	1.000	
a8	depr.	−10389/130	7.6	0.391	0.195/2
a9	opt.	−10550/14	0.0	1.000	
a9	prot.	−10534/60	0.0	1.000	
a9	depr.	−10362/108	7.2	0.2050	0.210/1

[a] The "opt." configuration has been generated using the MP2/6-31G** geometry optimized configuration of the acetic acid−water trimer, embedded in water, energy minimized and equilibrated for 40 ps. The "prot." and "depr." lines display averages over 5 simulations starting from random initial coordinates, each of them energy minimized and equilibrated for 40 ps in the protonated and in the deprotonated state, respectively. In the column "total energy", the total energy and its standard deviation is given. The reaction rate is the number of proton transfers between any oxygen atoms per picosecond, and the fraction of time the proton spends bound to the acetate ion is given as well. The average over 5 trajectories of the proton−oxygen distances after 1 ps for all five initial configurations is given only for the deprotonated state. The second number in the column "proton−oxygen dist." indicates the number of trajectories where the proton was captured by the acetate ion.

acceptor of the acid. Find the parameters σ_1 and ϵ_1 to reproduce the proton binding energy of the deprotonated state and the shape of the barrier.

7. Simulate the acid−water dimer in vacuo without thermostat starting from the ab initio configuration. If the potential energy fluctuates significantly, the shape of the potential function is not compatible with the minimum energy configuration, parameter σ_0 has to be adjusted, and step 7 has to be repeated. If the total energy fluctuates significantly, parameter σ_1 differs too much from σ_0 and has to be adjusted, and step 7 has to be repeated.

8. Do long MD proton transfer simulations starting from the randomly generated configurations of the solution.

9. If required, adjust the parameter qq to control the average distance between the proton and the proton acceptor and the proton return rate, and go back to step 6.

10. Do long QD/MD proton transfer simulations starting from the randomly generated solution configurations.

11. If required, adjust the parameters ϵ_0, ϵ_1, and r_1 to increase or to decrease the transfer rate and go back to step 7.

Note that the parameters for each protonizable compound should be found independently from the parameters for all other protonizable species. The parameters for the protonizable SPC/E water should not be changed without performing the tests for liquid water reported in ref 13.

IV. MD and QD/MD Simulations of Acetic Acid

The acetic acid−water trimer in vacuo has been simulated using several parameter sets for 5 ps. Too large a gap between the Lennard−Jones distance parameters σ_0 and σ_1 resulted in large fluctuations and even a drift of the total energy which could not be mitigated sufficiently by using a reduced time step or by applying softer-shaped potentials, such as 4−8 van der Waals instead of 6−12 van der Waals (Lennard−Jones) or a soft-core repulsive Lennard−Jones potential.[14] In Table 3, some results of MD simulations of proton transfers from and to acetic acid in water using different parameter sets are listed. No proton transfer from the acid molecule to a water molecule ever occurred, not even after 10 ps. The thermic energy of around $k_BT = 2.5$ kJ/mol (k_B is Boltzmann's constant, T is temperature) is not sufficient compared to the binding energy difference of about 700 kJ/mol between the proton bound to acetate and the proton bound to water. A swarm of trajectories starting from different random configurations, each of them energy minimized and equilibrated for 40 ps as described in step 2 of the procedure described in Section III, increased the configurational space sampled. Assuming a weak acid $[A^-] \ll [HA]$, the concentration $[H_3O^+]$ and the number $N_{H_3O^+}$ of hydronium ions depends on the acid's dissociation constant $K_a = 10^{-pK_a}$, the ion product of water $K_w = 10^{-pK_w}$, and the concentration $[HA]_0$ of the acid HA added initially to the water,

$$N_{H_3O^+} = N_A V_{box}[H_3O^+] = N_A V_{box}\sqrt{[HA]_0 K_a + K_w} = N_A V_{box}\sqrt{\frac{N_{HA_0}}{N_A V_{box}} K_a + K_w} \quad (20)$$

N_A being Avogadro's constant, V_{box} the volume of the system to be simulated, and $N_{HA_0} = 1$ the number of acid molecules in the simulated system. For acetic acid, $pK_a = 4.74$, and a box volume of 6.61867 nm^3 corresponding to 216 water molecules, the ion product of water can be neglected, and the average number of hydronium ions is 0.0085. The fraction of time the proton spends bound to the acetic acid is therefore 0.9915. While the time step for protonizable SPC/E water could be chosen as 0.25 fs,[13] 0.1 fs is required for acetic acid. One could think of two reasons for the obviously smaller potential function gradients in water: the proton transfers between water molecules occur when the potential function has approximately the shape of a single well, and the proton binding energies to all neighboring water molecules are intrinsically the same. Considering the dielectric permittivity of about 80 of liquid water and the involved kinetic energy of the proton, it is no surprise that the size of the monopole−monopole interaction constant qq has only little effect.[14]

In Table 4, experimental and computed heats of dissociation are compared for acetic acid in vacuo and in solution, and the heats of hydration are given for a proton. Using the protonizable SPC/E water model,[13] the deprotonated acetic acid is not stabilized by the second and further hydration shells due to the rigidity of the water molecules and, therefore, the heat of dissociation of acetic acid in solution is overestimated. To compensate this effect, the parameter ϵ_0 has been divided by two to obtain parameter set "a9" from set "a8". As Table 4 shows, the resulting values are closer to the measured range. In the infrared spectrum, the proton−oxygen stretch vibration can be associated with a very broad band between 3000 and 3600 cm^{-1}, and the corresponding band of proton bound carboxylic acids is seen around 3000 cm^{-1}, corresponding to periodic lengths of 11.1 and 9.2 fs, respectively.[25−27] From the Fourier transform of the trajectories of the distance between the proton and the oxygen atom, the periodic lengths of the proton−oxygen vibrations are around 20 fs for protonated SPC/E water and 2.2 fs for acetic acid, parameter set "a8". The latter value could be corrected by using a 4−8 van der Waals potential instead of 6−12, and again by decreasing the parameter ϵ_0. Using parameter set "a9", the periodic length of the proton−oxygen vibrations increases from 2.2 fs to 3.3 fs, and a side peak from simulations using set "a8" becomes the main peak at 20.0 fs which corresponds to roughly 1670 cm^{-1}, and is therefore due to the coupling to other vibrational modes.

Mixed QD/MD simulations of proton transfers using a one-dimensional representation of the quantum proton with many

TABLE 4: Heats ΔU and Enthalpies ΔH in kJ/mol Associated with Proton Transfer and Solvation Reactions from ab Initio and MD Calculations Compared to Experimental Values[a]

value	reaction	method	value	source
ΔH	$H^+(g) \rightarrow H^+(aq)$	various expt	−1126.6	[34]
ΔU	$H^+(g) \rightarrow H^+(aq)$	MD/fit-PSPC/E	−579.3	[13]
ΔU	$H^+(g) \rightarrow H^+(aq)$	MD/LJ-PSPC/E	−1876.8	[13]
ΔU	$H^+(g) \rightarrow H^+(aq)$	QD/MD/LJ-PSPC/E	−1879.2	[13]
ΔH	$HAc(g) \rightarrow H^+(g) + Ac^-(g)$	calorimetric	1445.6	[34]
ΔU	$HAc(g) \rightarrow H^+(g) + Ac^-(g)$	MP2/6-31G**	1548.7	Table 1
ΔH	$HAc(aq) \rightarrow H^+(aq) + Ac^-(aq)$	various expt	−0.4*	[34]
ΔU	$HAc(aq) \rightarrow H^+(aq) + Ac^-(aq)$	MD/a8	778.0*	Table 3
ΔU	$HAc(aq) \rightarrow H^+(aq) + Ac^-(aq)$	MD/a9	172.0*	Table 3

[a] The volume work per mol required for the phase change can be estimated assuming an ideal gas, $k_BT = 2.5$ kJ/mol at 300 K. The asterisk marks a very uncertain experimental value (the experimental enthalpy of dissociation of acetic acid in water at 298 K compiled in ref 33 varies from −0.6 to +8.0 kJ/mol) and a very uncertain computed value (see Section IV). The gas-phase kinetic energy of the proton $E_{kin}(H^+) = 3/2k_BT = 3.7$ kJ/mol has been taken into account for the calculation of the heats of hydration of a proton from the total energy values in Table 9 of ref 13, using Boltzmann's constant k_B and the temperature T.

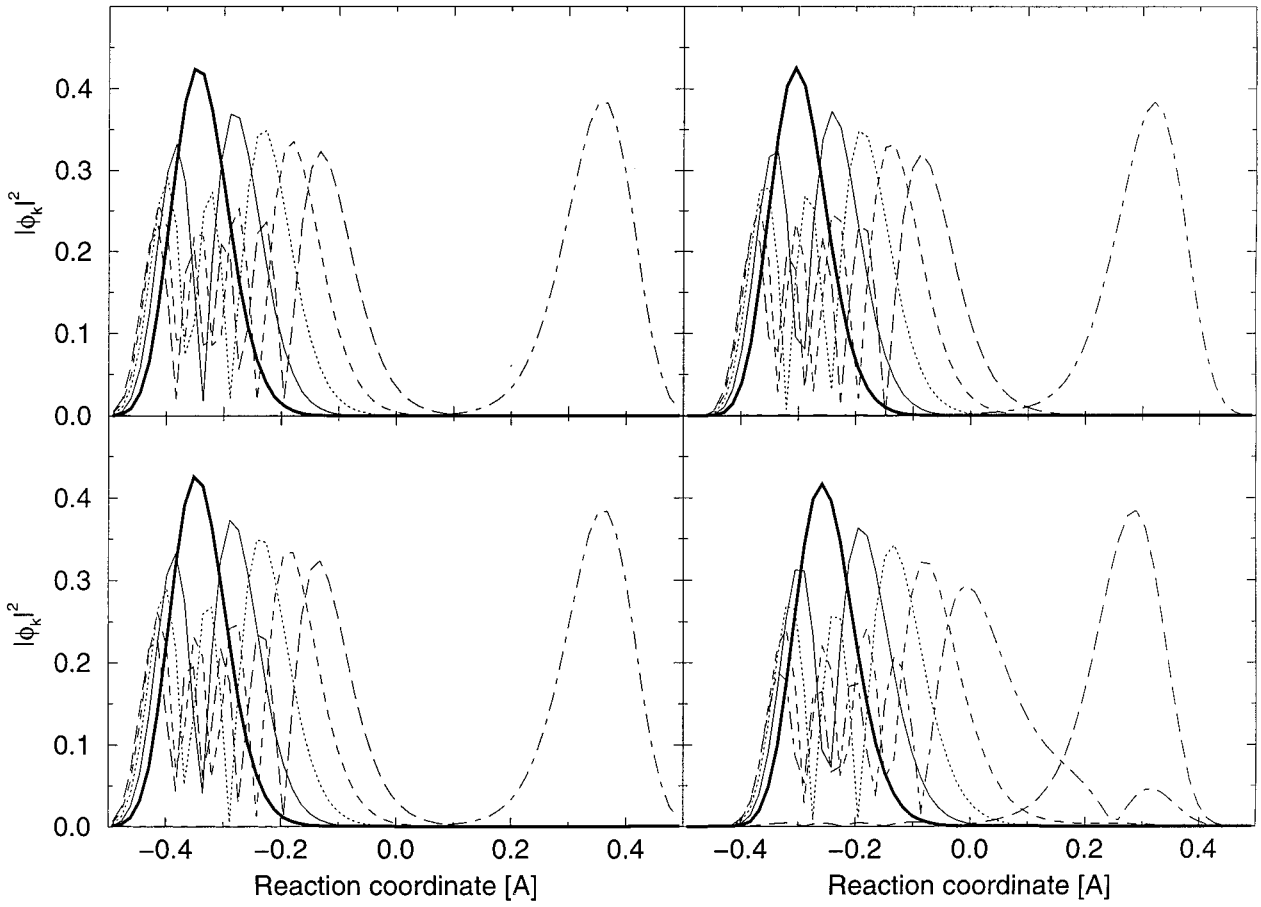

Figure 4. Eigenstates of the one-dimensional Hamilton operator of a proton bound to acetate and water, using the parameter set "a8". The basis consists of 64 equidistant points along the line connecting the atom O1 and the atom OW (see Figure 1). Top, left: acetic acid−water dimer, MP2/6-31G** geometry optimized configuration; top, right: acetic acid−water trimer, MP2/6-31G** geometry optimized configuration; bottom, left: acetic acid solvated in 216 water molecules; bottom, right: acetate ion and hydronium ion in 215 water molecules. The lines are as follows: ground (solid, thick), first excited (solid), second excited (dotted), third excited (dashed), fourth excited (long dashed), fifth excited (dot−dashed) state.

classical degrees of freedom are problematic even when avoiding the neglect of the force components to the proton perpendicular to the reaction coordinate.[13,15] However, due to their much smaller QD basis set, they are more handy than three-dimensional QD simulations and allow for a quick preview using various conditions. The first six energy eigenstates of the proton are shown in Figure 4 for two vacuum configurations and two configurations of acetic acid in solution. The gap between the eigenstates located close to the acid molecule and the one located close to the water molecule points at a potential barrier. It could be reduced by reducing the distance between the oxygen atom of the acid molecule and the oxygen atom of the nearest water molecule. The proton eigenstates of the solution configurations have been used as initial states for the QD/MD simulations whose results are listed in Table 5. The surprisingly large energies can be explained using Figure 5 which shows some snapshots of the proton potential energy function and the proton state out of trajectories, starting from the ground state and from the first excited state of the protonated configuration: For the ground state, the potential energy function becomes flat,

TABLE 5: QD/MD Simulations of Acetic Acid in 216 Water Molecules over 1 ps Using One Quantum Dimension and the Proton Potential Parameter set "a8" at 300 K starting from a Protonated ("prot.") and a Deprotonated ("depr.") Configuration ("Config." column) and from Different Energy Eigenstates of the Proton ("state" column)[a]

config.	state	total energy kJ mol^{-1}	potential energy kJ mol^{-1}	fraction of time	reaction rate ps^{-1}	encounters HAc 1/ps	net reactions
prot.	0	−1035/6037	−8559/2623	0.3773	279	89/0.9318	O1-w-O1-w-O1-O2-w
prot.	1	−6750/2357	−10743/1154	1.0000	0	1/1.0000	O1
prot.	2	625356/726760	34677/48575	0.4045	169	2/0.4205	O1-w-O2-w
prot.	3	−8427/1032	−11360/642	1.000	0	1/1.0000	O1
prot.	4	−7598/2135	−10898/1135	0.4385	52	19/0.4833	O1-w
depr.	0	−6140/1784	−10137/1009	0.2141	106	35/0.2726	O1-w-O1-w
depr.	1	−6617/1741	−10125/1167	0.3177	58	17/0.3539	O1-w-O1-w
depr.	2	−8721/957	−11376/570	0.5314	87	35/0.6217	O1-w-O1-w
depr.	3	−8080/967	−10961/622	0.2774	6	1/0.2774	O1-w

[a] In the columns "total energy" and "potential energy", the total and potential energy and their respective standard deviations are given. For the meaning of the columns "fraction of time" and "reaction rate" see Table 3. The reaction rate is the number of proton transfers between any oxygen atoms per picosecond, and the fraction of time the proton spends bound to the acetate ion is given as well. The number of proton transfers resulting in the acid being protonated and the time point in picoseconds of the last deprotonation of the acid are given in "encounters HAc". The remaining reactions after neglecting the back reactions and the proton transfers among water molecules are listed as "net reactions". The symbols O1 and O2 denote the proton acceptor oxygen atom (see Figure 1), and "w" denotes proton transfers among water molecules.

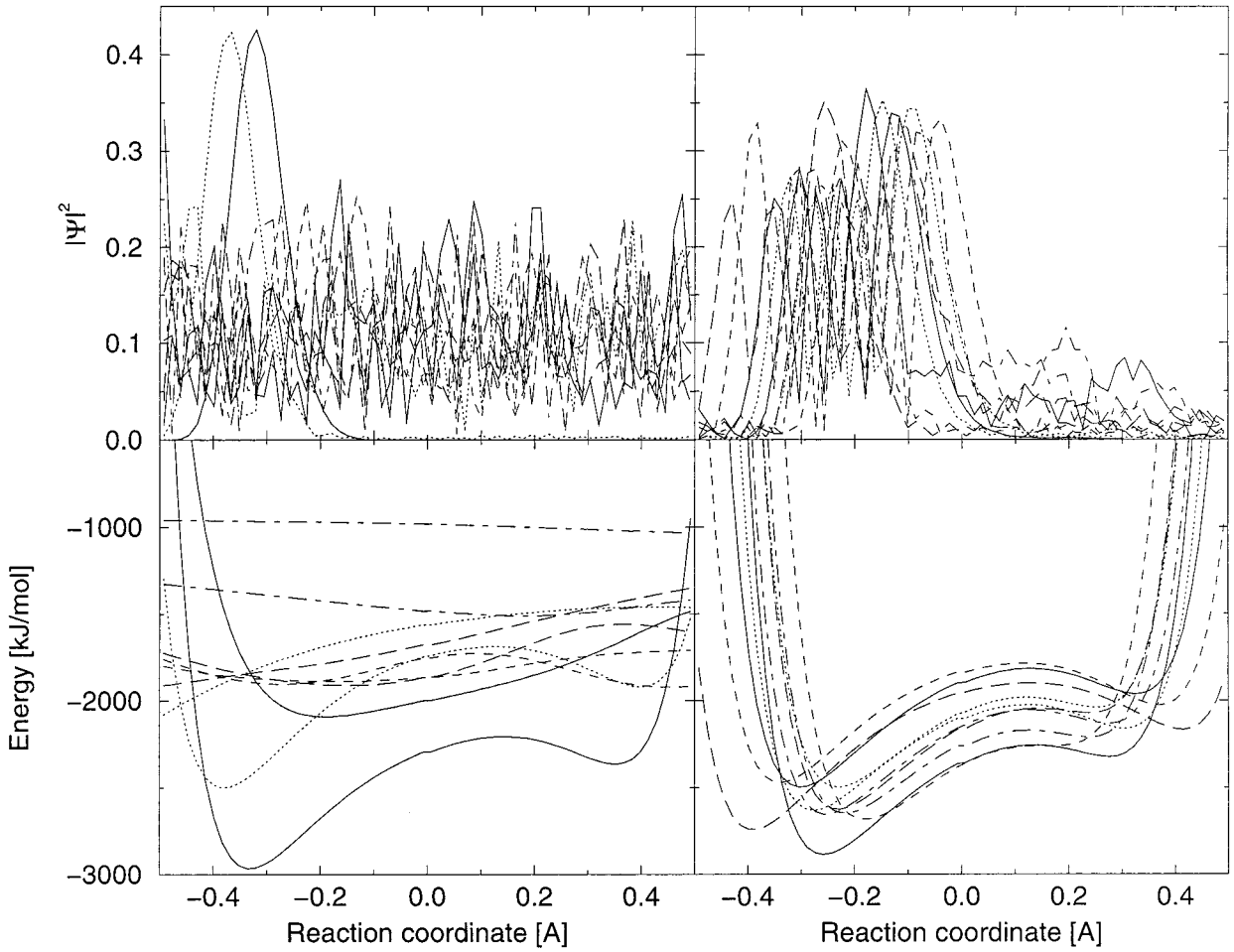

Figure 5. Trajectories of a QD/MD simulation of acetic acid in 216 water molecules over 1 ps, using the parameter set "a8". Snapshots of the QD state function and the potential energy function have been taken every 0.1 ps. The proton has been described quantum dynamically using 64 grid points in one dimension between the atom O1 and the atom OW (see Figure 1) as basis functions. The lines represent: 0.1 and 0.2 ps (solid lines), 0.3 and 0.4 ps (dotted lines), 0.5 and 0.6 ps (dashed lines), 0.7 and 0.8 ps (long dashed lines), 0.9 and 1.0 ps (dot−dashed lines). Top row: absolute square of the state function; bottom row: potential energy function; left side: starting from the proton ground state; right side: starting from the proton first excited state.

indicating that the proton transfer reaction coordinate does not coincide anymore with the line on which the basis points are located. This happens, for example, when the oxygen atom of another water molecule is approaching this line. The results are a noisy state and unpredictable numbers. The trajectories starting from the protonated configuration and from the first excited state show reasonable behavior (see Figure 5 and Table 5).

Such problems are not to be expected from simulations using a three-dimensional representation of the quantum proton. In Table 6, the average occupation numbers of the lower energy eigenstates are compared against the ones to be expected from a canonical ensemble, and a graphical representation of the energy eigenvalues and the population of the adiabatic states can be found in Figure 6. Compared to the canonical ensemble,

TABLE 6: QD/MD Simulations of a Proton in 216 Water Molecules ("SPC/E") and of Acetic Acid in 216 Water Molecules ("HAc") over Different Time Periods in picoseconds Using Three Quantum Dimensions and the Proton Potential Parameter Set "a8" at 300 K Starting from a Classically Optimized and Equilibrated Configuration and from Different Adiabatic States of the Proton[a]

system	state	time	E_{tot}/E_{pot}	$\|\langle k\|\Psi\rangle\|^2$ (sim.)	$\|\langle k\|\Psi\rangle\|^2$ (expt)
HAc	12/0	0.1	−10953/−12710	0.461/0.170/0.077/0.093	0.993/0.006/0.001/0.000
HAc	12/0	0.2	−10620/−12643	0.366/0.112/0.113/0.076	0.986/0.012/0.002/0.000
HAc	16/0	0.1	−10969/−12713	0.523/0.159/0.074/0.084	0.994/0.005/0.001/0.000
HAc	16/0	0.2	−10927/−12707	0.474/0.130/0.088/0.084	0.994/0.005/0.001/0.000
HAc	16/1	0.1	−10847/−12675	0.253/0.176/0.031/0.067	(0.991/0.006/0.002/0.000)
HAc	16/2	0.1		0.040/0.113/0.259/0.130	(0.994/0.005/0.001/0.000)
HAc	16/3	0.1		0.053/0.112/0.077/0.128	(0.992/0.006/0.002/0.000)
SPC/E	16/0	0.1	−9704/−11411	0.908/0.021/0.040/0.010	0.999/0.001/0.000/0.000
SPC/E	16/0	0.2	−9938/−11620	0.875/0.032/0.038/0.017	0.999/0.001/0.000/0.000
SPC/E	16/0	0.3	−9933/−11620	0.791/0.049/0.044/0.033	0.999/0.000/0.000/0.000
SPC/E	16/0	1.0	−9705/−11411	0.388/0.066/0.049/0.038	0.999/0.001/0.000/0.000
SPC/E	18/0	0.1	−9944/−11618	0.908/0.021/0.040/0.010	0.999/0.001/0.000/0.000
SPC/E	18/0	0.2	−9938/−11621	0.879/0.031/0.035/0.016	0.999/0.001/0.000/0.000
SPC/E	18/0	0.3	−9934/−11621	0.793/0.050/0.044/0.032	0.999/0.000/0.000/0.000
SPC/E	18/0	1.0	−9675/−11377	0.412/0.057/0.054/0.044	0.998/0.002/0.000/0.000

[a] The column "state" contains the number of grid points along one dimension (N_{ptd}) and the number of the initial state (0 represents the ground state). The averaged total (E_{tot}) and potential (E_{pot}) energies are given in kJ/mol. The averaged occupation numbers $|\langle k|\Psi\rangle|^2$ obtained from the QD/MD simulations "(sim.)" are compared to the averaged occupation numbers to be expected from the proton energy eigenvalues assuming a canonical ensemble "(exp.)". See also Figure 6.

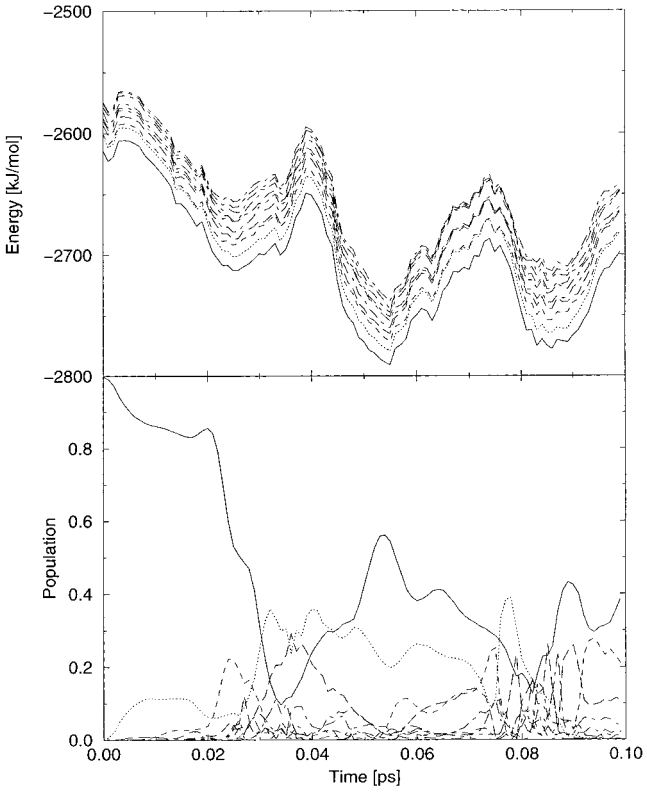

Figure 6. Trajectories of a QD/MD simulation of acetic acid in 216 water molecules over 0.1 ps, using the parameter set "a8" and a three-dimensional representation of the proton state with 12 grid points in each dimension. The simulation has been started from the proton ground state (see also Table 6). Top: Energies of the ten lowest adiabatic states of the proton; bottom: population (absolute square of the expansion coefficients) of the same states as in the top graph. The lines represent: ground state (solid), first (dotted), second (dashed), third (long dashed), and all higher (dot−dashed) excited states.

the excited states are overpopulated, and further investigations must show if too small a basis set is the source of the heat causing the overpopulation of the excited states. These investigations using a much larger basis set require an efficient potential energy interpolation scheme, as can be seen from Table 7. The incorporation of surface hopping techniques[19,28] into QDGROMOS is planned and does not impose any computational overhead since the Hamiltonian of the proton is also diagonalized in QDGROMOS.[15] From the one-dimensional simulations it is clear that not more than 32 points in each dimension are required.

TABLE 7: User CPU Time (in seconds, Required for One MD or QD/MD Integration Time Step on a DEC Alpha 21164, 600 MHz, Given for Various Systems, Representations of the Proton State (N_{dqm} is the number of dimensions, and N_{ptd} is the number of grid points in each dimension), and Diagonalization Techniques of the Hamiltonian ("Eigensolver")[a]

system	number of waters	N_{dqm}	N_{ptd}	Eigensolver	user CPU
acetic acid	1	3	16	JD	83.0
acetic acid	216	MD			0.28
acetic acid	216	1	64	QR	3.90
acetic acid	216	3	12	QR	584.3
acetic acid	216	3	12	JD	133.9
acetic acid	216	3	16	JD	350.2
water	216	3	16	JD	338.9
water	216	3	18	JD	343.0

[a] "QR" refers to the traditional QR decomposition, and "JD" to a derivative of the Jacobi−Davidson method.[35]

V. Free Energy Profile of a Proton Transfer Reaction

A. Umbrella Sampling and Thermodynamic Integration. If one state of protonation is much less populated in equilibrium than the other one, the proton transfer reaction can neither be simulated directly nor is the configuration space sufficiently sampled near the transition state in order to obtain a free energy profile of the reaction. Umbrella sampling is an established method for enhancing the sampling near a known reaction path.[29,30] A restraint function, in our case a partially harmonic distance restraint,

$$V_{umb}(r) = \begin{Bmatrix} \frac{1}{2}k_{umb}(r - r_{umb})^2 & \text{if } r - r_{umb} \le \Delta r_{umb} \\ k_{umb}\Delta r_{umb}\left(r - r_{umb} - \frac{1}{2}\Delta r_{umb}\right) & \text{if } r - r_{umb} > \Delta r_{umb} \end{Bmatrix} \quad (21)$$

is added to the Hamiltonian in the simulation.[11] The force constant k_{umb}, the reference distance r_{umb}, and the threshold distance Δr_{umb} are used as parameters. More generally, the umbrella potential $V_{umb}(\lambda,\lambda_i)$ is expressed in terms of a reaction coordinate λ and the parameter λ_i which is varied for several MD simulations such that the entire reaction path is sampled. With the adjustable constant C', the free energy

$$F(\lambda) = -k_B T \ln P(\lambda) + C' \tag{22}$$

depends on the unbiased probability $P(\lambda)$ of finding the reaction coordinate at the value λ, which in turn can be derived from the probability $P_{umb}(\lambda,\lambda_i)$ obtained using $V_{umb}(\lambda,\lambda_i)$,

$$P(\lambda) = P_{umb}(\lambda,\lambda_i) \times \exp(V_{umb}(\lambda,\lambda_i)/k_B T) \times C''_{\lambda_i} \tag{23}$$

The constants C_{λ_i} in

$$F(\lambda) = -k_B T \ln P_{umb}(\lambda,\lambda_i) - V_{umb}(\lambda,\lambda_i) + C_{\lambda_i} \tag{24}$$

can be chosen such that $F(\lambda)$ is a continuous function for all λ_i. In the case of QD/MD, the probability $P_{umb}(\lambda,\lambda_i)$ depends also on the state $|\Psi\rangle$.

Compared to other force field terms, the potential energy differences arising from proton transfers are large, and the force constant k_{umb} must be chosen accordingly. It is important that the simulations start from configurations which have been thoroughly equilibrated using a sufficiently large force constant k_{umb} for each λ_i, since the environment stabilizes a state of protonation considerably. Therefore, the force constants can be relaxed after the equilibration. If the resulting probability distributions are still too narrow, multiconfigurational thermodynamic integration[31] can be applied to find the free energy difference of the reaction,

$$\Delta F = \sum_i \left\langle \frac{\partial \hat{H}}{\partial \lambda} \right\rangle_{\lambda_i} \times \Delta\lambda_i \tag{25}$$

using the unbiased Hamiltonian $\hat{H}$ and the intervals $\Delta\lambda_i$. When neglecting entropic contributions due to $\partial S/\partial\lambda$ at a local maximum λ_{max} of a biased probability function,

$$\left| T \times \frac{\partial S(\lambda_{max})}{\partial \lambda} \right| \ll |f_{umb}(\lambda_{max})| \tag{26}$$

the restraint force $f_{umb}(\lambda_{max})$ equals the opposite of the average force along the reaction coordinate,

$$f_{umb}(\lambda_{max}) = \left\langle \frac{\partial \hat{H}}{\partial \lambda} \right\rangle_{\lambda_{max}} \tag{27}$$

Since the restraint force is harmonic, its size is determined by the value of $\lambda_{max} - \lambda_i$, and only the values λ_{max} have to be known in order to obtain a free energy profile of the reaction in this case.

B. Results. The free energy profiles of the proton transfer reaction between acetic acid and water in solution resulting from umbrella sampling and thermodynamic integration using the same trajectories are shown in Figure 7. Note that the distance between the proton and the acetate ion is not the reaction coordinate itself but has been chosen as a representative of a collective coordinate.[32] Another common approach is to let the energy difference between the two reference states represent the reaction coordinate. The free energy of dissociation using parameter set "a8" is $\Delta F = 545$ kJ/mol using umbrella sampling

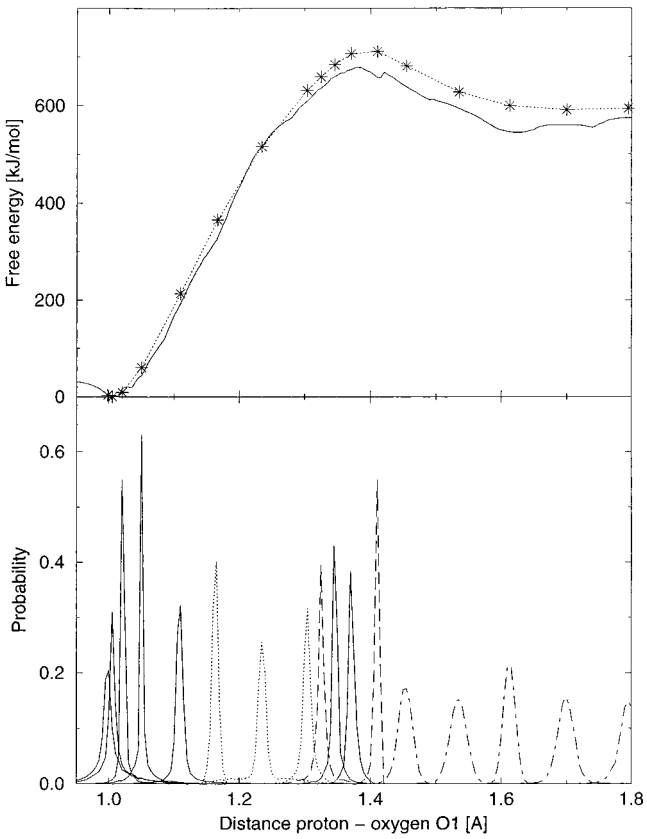

Figure 7. Free energy of the proton transfer between acetic acid (oxygen atom O1) and one water molecule (oxygen OW, see Figure 1) solvated in 216 water molecules using periodic boundary conditions and parameter set "a8", as function of the distance between the proton and the oxygen atom O1. The system has been equilibrated for 40 ps using a force constant of $k_{umb} = 5.0 \times 10^6$ kJ/(mol nm^2) for each reference distance r_{umb}, and the configurational space has been sampled for another 40 ps using force constants of $k_{umb} = 1.5 \times 10^6$, $k_{umb} = 3.0 \times 10^6$, $k_{umb} = 5.0 \times 10^6$, and $k_{umb} = 8.0 \times 10^6$ kJ/(mol nm^2). The reference distances have been (from left to right) 0.95, 1.0, 1.1, 1.2, 1.3, 1.25, 1.3, 1.35, 1.35, 1.36, 1.38, 1.4, 1.4, 1.5, 1.6, 1.7, and 1.8 Å. Top: Free energy obtained using umbrella sampling (solid line) and thermodynamic integration (dotted line and stars). The same raw data have been used for both lines. Bottom: Probability distributions resulting from different reference distances r_{umb} and force constants k_{umb}.

and 591 kJ/mol using thermodynamic integration, compared to the heat of dissociation $\Delta U = 778$ kJ/mol for the same parameter set (Table 4). The similarity of the two profiles shows that knowing only the values λ_{max} is sufficient to obtain a free energy profile. From the $pK_a = 4.74$ and the resulting probability of the protonated state 0.9915 (see Section IV), the free energy difference between the protonated state *d* and the deprotonated state *p*

$$\Delta F_{p\rightarrow d} = -k_B T \times \ln\left(\frac{P_d}{P_p}\right) \tag{28}$$

is expected to be 11.87 kJ/mol. Note that this value cannot be compared to the free energy profile in Figure 7, since some entropic contributions to the proton transfer between an acetate ion and *all* water molecules are not accounted for in the proton transfer between an acetate ion and *one* water molecule. The free energy of the proton transfer can be expected to be much smaller when using parameter set "a9" instead of "a8", see Table 4: $\Delta U = 778$ kJ/mol using set "a8" and 172 kJ/mol using set "a9".

VI. Conclusions and Outlook

With novel empirical force field terms in a mixed quantum dynamics/molecular dynamics framework, the dynamics of proton transfer to acetic acid in solution was simulated. A general procedure for finding hydrogen bond potential parameters was presented. Simulations were started from several independent initial configurations to enhance the sampling, which is otherwise limited due to the short integration time step of 0.1 fs. A free energy profile of a proton transfer reaction in solution has been calculated using pure MD only. The MD and QD/MD simulation machinery have been tested sufficiently to allow proton transfer simulations in large biomolecules such as (solvated) proteins. For the appropriate description of the quantum dynamics of a proton represented in three dimensions in a biochemical environment, using more than 18 points in each dimension and an efficient proton potential energy interpolation scheme are required.

References and Notes

(1) Bicout, D., Field, M., Eds.; *Quantum mechanical simulation methods for studying biological systems*; Heidelberg and Les Ulis, Les Editions de Physique: Springer, New York, 1996.

(2) Grochowski, P.; Lesyng, B.; Bala, P.; McCammon, J. A. *Intl. J. Quant. Chem.* **1996**, *60*, 1143.

(3) Tuckerman, M. E.; Laasonen, K.; Sprik, M.; Parrinello, M. *J. Chem. Phys.* **1995**, *103*, 150.

(4) Laasonen, K.; Sprik, M.; Parrinello, M. *J. Chem. Phys.* **1993**, *99*, 9080.

(5) Halley, J. W.; Rustad, J. R. *J. Chem. Phys.* **1993**, *98*, 4110.

(6) Duh, D.-M.; Perera, D. N.; Haymet, A. D. J. *J. Chem. Phys.* **1995**, *102*, 3736.

(7) Åqvist, J.; Warshel, A. *Chem. Rev.* **1993**, *93*, 2523.

(8) Lobaugh, J.; Voth, G. A. *J. Chem. Phys.* **1996**, *104*, 2056.

(9) Vuilleumier, R.; Borgis, D. *J. Chem. Phys.* **1999**, *111*, 4251.

(10) Schmitt, U. W.; Voth, G. A. *J. Phys. Chem. B* **1998**, *102*, 5547.

(11) van Gunsteren, W. F.; Billeter, S. R.; Eising, A. A.; Hünenberger, P. H.; Krüger, P.; Mark, A. E.; Scott, W. R. P.; Tironi, I. G. *Biomolecular Simulation: The GROMOS96 Manual and User Guide*; Biomos b.v., Zürich and Groningen, VdF Hochschulverlag, ETH Zürich, Zürich, 1996.

(12) Scott, W. R.P.; Hünenberger, P. H.; Tironi, I. G.; Mark, A. E.; Billeter, S. R.; Fennen, J.; Torda, A. E.; Huber, T.; Krüger, P.; van Gunsteren, W. F. *J. Phys. Chem. A* **1999**, *103*, 3596.

(13) Billeter, S. R.; van Gunsteren, W. F. *J. Phys. Chem.* **1998**, *102*, 4669.

(14) Billeter, S. R. *Quantum dynamical simulation of non-adiabatic proton transfers in aqueous solution: methodology, molecular models and applications*, Ph.D. Thesis, ETH Zürich, 1998, Diss. ETH 12751.

(15) Billeter, S. R.; van Gunsteren, W. F. *Comput. Phys. Commun.* **1997**, *107*, 61.

(16) Bala, P.; Grochowski, P.; Lesyng, B.; McCammon, J. A. *Comput. Chem.* **1995**, *19*, 155.

(17) Mavri, J.; Berendsen, H. J. C. *J. Phys. Chem.* **1995**, *99*, 12711.

(18) Drukker, K.; Hammes-Schiffer, S. *J. Chem. Phys.* **1997**, *107*, 363.

(19) Tully, J. C. *J. Chem. Phys.* **1990**, *93*, 1061.

(20) Sun, X.; Miller, W. H. *J. Chem. Phys.* **1997**, *106*, 916.

(21) Prezhdo, O. V.; Rossky, P. J. *J. Chem. Phys.* **1997**, *107*, 825.

(22) Frisch, M. J.; Trucks, G. W.; Schlegel, H. B.; Gill, P. M. W.; Johnson, B. G.; Robb, M. A.; Cheeseman, J. R.; Keith, T.; Petersson, G. A.; Montgomery, J. A.; Raghavachari, K.; Al-Laham, M. A.; Zakrzewski, V. G.; Ortiz, J. V.; Foresman, J. B.; Cioslowski, J.; Stefanov, B. B.; Nanayakkara, A.; Challacombe, M.; Peng, C. Y.; Ayala, P. Y.; Chen, W.; Wong, M. W.; Andres, J. L.; Replogle, E. S.; Gomperts, R.; Martin, R. L.; Fox, D. J.; Binkley, J. S.; Defrees, D. J.; Baker, J.; Stewart, J. P.; Head-Gordon, M.; Gonzalez, C.; Pople, J. A. *Gaussian 94, Revision C.3*; Gaussian, Inc., Pittsburgh, PA, 1995.

(23) Berendsen, H. J. C.; Postma, J. P. M.; van Gunsteren, W. F.; DiNola, A.; Haak, J. R. *J. Chem. Phys.* **1984**, *81*, 3684.

(24) *Maple V release 3*; Waterloo Maple Software, Waterloo, 1994.

(25) Weidlein, J.; Müller, U.; Dehnicke, K. *Schwingungsspektroskopie*; Thieme Verlag: Stuttgart and New York, 1982.

(26) Flett, M. S. C. *Characteristic frequencies of chemical groups in the infra-red*; Elsevier: Amsterdam and London and New York, 1963.

(27) Flett, M. S. C. *J. Chem. Soc.* **1951**, 962.

(28) Hammes-Schiffer, S.; Tully, J. C. *J. Chem. Phys.* **1995**, *103*, 8528.

(29) Torrie, G. M.; Valleau, F. P. *J. Comput. Phys.* **1977**, *23*, 187.

(30) *Computer simulation of biomolecular systems*; volume 2, part IV; van Gunsteren, W. F., Weiner, P. K., Wilkinson, A. J., Eds. Escom: Leiden, 1993; pp 267−367.

(31) Straatsma, T. P.; McCammon, J. A. *J. Chem. Phys.* **1991**, *95*, 1175.

(32) Ando, K.; Hynes, J. T. *J. Mol. Liq.* **1995**, *64*, 25.

(33) Christensen, J. J.; Hansen, L. D.; Izatt, R. M. *Handbook of proton ionisation heats and related thermodynamic quantities*; John Wiley & Sons: New York, 1976.

(34) Wilson, B.; Georgiadis, R.; Bartmess, J. E. *J. Am. Chem. Soc.* **1991**, *113*, 1762.

(35) Strebel, R.; Arbenz, P.; Gander, W.; Billeter, S. R.; van Gunsteren, W. F., in preparation.